Defence Science Journal, Vol. 72, No. 3, May 2022, pp. 326-333, DOI : 10.14429/dsj.72.3.17040
© 2022, DESIDOC

Numerical and Experimental Investigation of a Short-Recoil-Operated Weapon and Impact of Construction Characteristics on its Operation Cycle

Przemysław Badurowicz,[#,*] Przemysław Kupidura[$] and Bartosz Fikus[$]

[#]*Military Institute of Armament Technology, 7 Prymasa Stefana Wyszyńskiego Street, 05-220 Zielonka, Poland*
[$]*Faculty of Mechatronics, Armament and Aerospace, Military University of Technology, 2 Sylwestra Kaliskiego Street, 00-908 Warsaw, Poland*
[*]*E-mail: badurowiczp@witu.mil.pl*

ABSTRACT

Estimation of kinematic and dynamic parameters of weapon mechanisms during operation is one of the crucial elements of design and optimisation. This study presents results of numerical and experimental investigations of a short-recoil-operated weapon action cycle. Theoretical considerations were based on multibody systems and finite element approaches. An experimental stand was adopted to investigate the kinematic characteristics of pistol parts and provide a set of slide displacement and velocity time courses. Comparison of theoretical and experimental data allowed for positive validation of the investigated model. The multibody systems numerical approach ensured a maximum relative discrepancy with experiment of 3.5 per cent for the velocity of recoiled parts, while finite element analysis calculations yielded a value of 12.7 per cent. Finally, parametric analyses were conducted to determine the influence of selected design characteristics on weapon operation. The analyses proved the correctness of the adopted design assumptions.

Keywords: Mechanics; Numerical investigation; Multibody systems; Finite element analysis; Kinematic characteristics; Weapon design; Short-recoil operation; Parametric investigation

NOMENCLATURE

C	Sound speed in the material
C_{cont}	Damping coefficient
CFL	Time step safety factor ($CFL < 1$ (~0.8–0.9) for slowly changing phenomena)
d	Contact coefficient or penetration depth
D	Depth of penetration
e	Contact coefficient or force exponent
F	Total force acting on the centre of mass
F_0	Static force of interaction between projectile and case
F_{01}	Dynamic force of interaction between projectile and case
F_{bb}	Force of bullet engraving the barrel
F_{bc}	Force of extracting bullet from case
F_{cont}	Normal contact force
F_{ec}	Forces of extraction and ejection of case
F_{es}	Force of extractor spring
F_{fc}	Force of feeding and chambering of the next cartridge
F_m	Force of mainspring
F_{ms}	Force of magazine spring
F_p	Force of gas pressure acting on the bottom of the case
F_{rs}	Force of recoil spring
F_{sd}	Force of interaction between the slide and the disconnector
F_{sh}	Force of interaction between the slide and the hammer
F_{tb}	Force of trigger bar spring
h	Element characteristic dimension
I	Identity matrix
J_c	Moment of inertia about the centre of mass
k_{cont}	Coefficient of stiffness
L	Lagrangian function
l_{dpb}	Depth of pressed bullet into case
m	Mass of the body
M_F	Effective mass of the face
M_N	Effective mass of the node
N_c	Total torque acting about the centre of mass
Q	Generalised forces
t_{bo}	Breech opening time, from the beginning of the slide motion to the complete lowering of the barrel
t_{ej}	Cartridge case ejection time, from the moment when the barrel loses contact with the cartridge case to the moment when the case hits the ejector
t_{ex}	Cartridge case extraction time, from the complete lowering of the barrel to the moment when the barrel loses contact with the cartridge case

Received : 11 May 2021, Revised : 12 April 2022
Accepted : 29 April 2022, Online published : 01 July 2022

t_f	Time of slide forward motion
t_r	Time of slide recoil
v	Relative sliding velocity at point of contact
$\bar{V}_c$	Acceleration of the centre of mass
$v_{f\max}$	Maximum velocity of slide forward motion
$v_{r\max}$	Maximum velocity of slide recoil
v_{sb}	Velocity of slide impact to buffer
β	Exponential decay coefficient
Δt	Time step
Δt_{bo}	Change in breech opening time relative to nominal
Δt_{ej}	Change in cartridge case ejection time relative to nominal
Δt_{ex}	Change in cartridge case extraction time relative to nominal
Δt_f	Change in average time of slide forward motion relative to nominal
Δt_r	Change in time of slide recoil relative to nominal
$\Delta v_{f\max}$	Change in maximum velocity of slide forward motion relative to nominal
$\Delta v_{r\max}$	Change in maximum velocity of slide recoil relative to nominal
Δv_{sb}	Change in velocity of slide impact to buffer relative to nominal
λ	Lagrange multiplier
μ	Friction coefficient
μ_d	Dynamic friction coefficient
μ_s	Static friction coefficient
ϕ	Constraint conditions
ω	Angular velocity of the body
$\bar{\omega}$	Angular acceleration of the body
$[C]$	Damping matrix
$[F]$	Force matrix
$[K]$	Stiffness matrix
$[M]$	Mass matrix
$\left[u\right]$	Node displacement matrix
$\left[\bar{u}\right]$	Node velocity matrix
$\left[\bar{\bar{u}}\right]$	Node acceleration matrix
$\square$	Skew-symmetric cross-product matrices

1. INTRODUCTION

Numerical simulations of mechanical systems are currently at a crucial stage in the design and optimisation or failure analysis, especially in armament development. The growing number of available reports in this field confirms the interest of research groups in application of numerical analysis and available software in weapons technology. An interesting example of a possible numerical approach implementation in optimizing the construction of a relatively new weapon (the 5.56 mm MSBS-5.56 rifle) was described in Damaziak, *et al.*[1]. Damaziak, *et al.* presented the option of using finite element analysis (FEA) (and the finite element method (FEM)) and multibody analysis (MBA) (and multibody systems (MBS)) approaches in automatic rifle construction optimisation and failure spot determination. The investigation results were compared to the data recorded during experimental tests. A similar approach to the simulation of gun element motion was considered by Fikus and Trębiński[2], who presented the results of submachine gun multibody simulations, which allowed for indirect validation of an additional interior ballistics model[3]. Other researchers[4-6] conducted simplified numerical simulations and experimental investigations of rifle jump, additionally suggesting some ways for its reduction. Their considerations were positively validated by a large amount of experimental data. Ni., *et al.*[7] developed and calculated the MBS model in MSC Adams software and validated it. Rodriguez[8] presented a numerical model and results of investigation and experimental tests on the XM307 Advanced Crew Served Weapon. Benelli[9] presented the potential of using MSC Adams for shotgun design and calibrated the presented model with experimental data (i.e., the model parameters were adjusted to obtain compatibility between theoretical and experimental results). Ozmen, *et al.*[10] presented fatigue analyses of a weapon locking block. Hopkins[11] put forward models that use beam theory to describe the mutual influence of a gun system–projectile. Because the approach was formulated using beam elements), it provides high computational efficiency. The results of the numerical investigation were supplemented by experimental data.

This study is a continuation of that given in reference 12, where a preliminary rigid-body model of a short-recoil-operated pistol was considered. The multibody model was improved by adding more accurate forces applied to the weapon parts, and the analyses were supplemented by FEA and MBS parametric analyses and experimental investigations of real pistol characteristics. The more accurate forces included the force of extracting the bullet from the case and the force of the bullet engraving the barrel. The other forces (as described in Badurowicz, *et al.*[12]) were the force of gas pressure and spring forces. A parametric investigation allowed us to prove the correctness of weapon operation.

2. NUMERICAL MODELS

2.1 MBA Numerical Model

In the MBA, system parts are assumed to be rigid and are connected by kinematic pairs of different classes. Bodies move under the action of forces and torques (e.g., internal and external forces, concentrated and distributed forces, and contact forces with or without friction).

The equations of motion can be formulated in general coordinates, most often using the Lagrange equations[13].

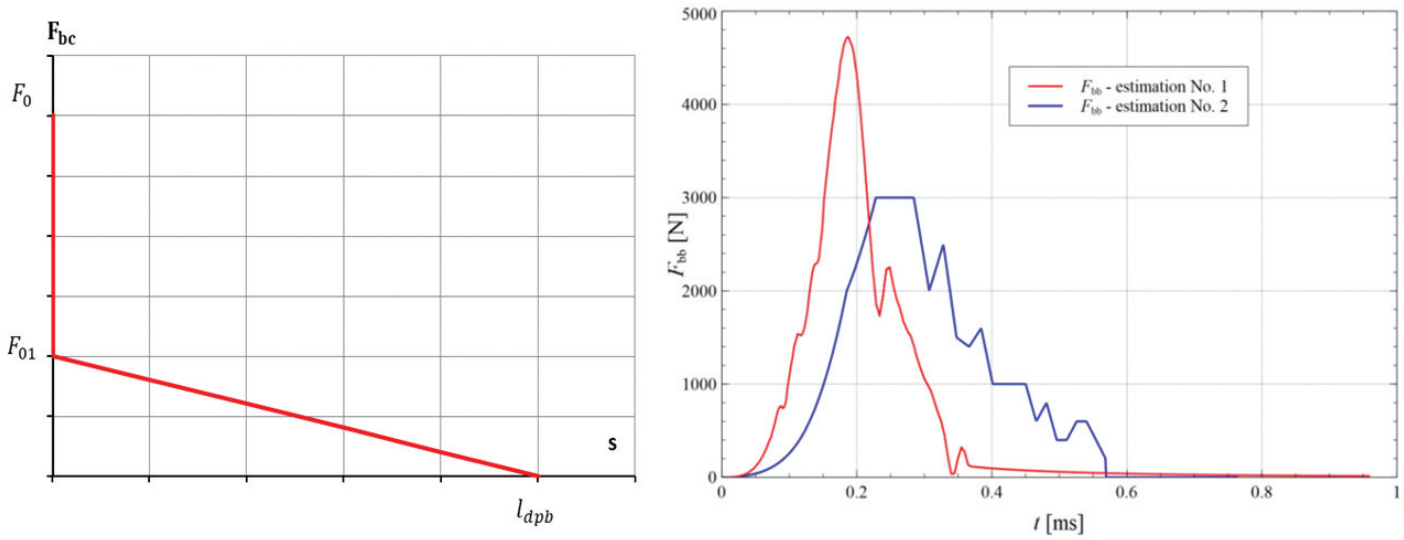

Figure 1. Estimated forces acting on parts. (a) Qualitative curve of force extracting bullet from case F_{bc} versus displacement of bullet[3]. Force of bullet engraving the barrel (F_{bb}) versus time for 9×19 mm Parabellum projectile: estimation No. 1—in accordance with[3]; estimation No. 2—in accordance with[15].

$$\frac{d}{dt}\left(L_q^T\right) - L_q^T + \phi_q^T \lambda = Q \tag{1}$$

Another possible formulation of the problem is to use the Newton–Euler equations[13].

$$\begin{bmatrix} mI & 0 \\ 0 & J_c \end{bmatrix} \begin{bmatrix} \dot{V}_c \\ \dot{\omega} \end{bmatrix} + \begin{bmatrix} 0 \\ \omega J_c \omega \end{bmatrix} = \begin{bmatrix} F \\ N_c \end{bmatrix} \tag{2}$$

2.2 MBS Numerical Model

The preliminary MBS numerical model was developed as described in Badurowicz *et al.*[12]. The system was loaded with the following forces: F_p, F_{rs}, F_m, F_{ms}, F_{tb}, F_{es}, F_{bc}, and F_{bb}. The following initial and boundary conditions were specified:

- Parts of the pistol (rigid elements) are stationary at the initial moment $t = 0$.
- Material parameters are defined for the parts.
- The forces acting on the system are defined.
- At the initial moment $t = 0$, the gas pressure starts to increase.
- The following stationary parts during a shot are fixed in the numerical model: the grip module, frame, magazine box, barrel disconnector, and takedown pin.
- The number of degrees of freedom is determined for the parts.
- A total of 21 contact pairs are defined.

The external force causing parts to move is the propellant gas pressure force, obtained experimentally from 10 shots. The tests were performed for 9×19 mm Parabellum ammunition with a lead core (Mesko S.A., Poland).

The preliminary model presented in Badurowicz *et al.*[12] was significantly improved. In this work, the model was supplemented with more accurately estimated forces of extracting the bullet from the case and the bullet engraving the barrel rifling bore (Fig. 1).

The force extracting the bullet from the case (F_{bc}) for the 9×19 mm cartridge, according to the STANAG 4090, should be ≥200 N. In accordance with[3], this force (F_{bc}) (Fig. 1a) is ~600 N (F_0) when the projectile does not move (for static friction). When the bullet starts its motion (dynamic friction), the force decreases to a value of 200 N (F_{01}) and it tends linearly to zero until the bullet and the case completely disintegrate. The depth of the projectile pressing into the case (l_{dpb}) is 5.65 mm. This model of extracting the bullet from the case (F_{bc}) was adopted in this study.

The force of the bullet engraving the barrel bore (F_{bb}) was adopted from Fikus *et al.*[3] (Fig. 1b), who obtained this force using the FEM. Other studies[14-15] on this subject are less useful because they do not indicate an explicit value for the interaction force between a projectile and a barrel under dynamic conditions. The measurement of the force in quasi-static conditions as done by South, *et al.*[14] is not applicable in this case because of the extremely dynamic character of the analysis. Kowalczyk, *et al.*[15] presented the total value of the energy needed to extract the bullet from the case and for the bullet to engrave the barrel. For the purposes of this study, the force was calculated using differentiation (Fig. 2b). The forces according to Refs.[3,15] are different, but the impulses are very similar, which proves that both estimates are reliable. The force increases with increasing gas pressure at the beginning of the projectile motion. Its maximum occurs at the moment of maximum gas pressure, and then the force decreases until it reaches a value of zero when the bullet leaves the barrel.

According to Fikus and Trębiński[2], a time step of 50 μs gives acceptable results. In this study, a time step of 31.5 μs was used. Further reduction of the time step changes the results marginally.

2.3 FEM Numerical Model

Two FEM numerical models were developed in Ansys software. The first is the basic one, in which the interaction forces between the slide and the hammer and between the slide and the disconnector and the forces of extraction and ejection

of the spent case, as well feeding and chambering of the next cartridge, are all ignored. The second model was extended by adding the above-mentioned forces, which were estimated using MBA. Development of both FEM numerical models included simplifications to the geometric complexity and number of parts, which resulted in a noticeable reduction of the number of elements. The materials applied in FEA simulations were assumed to be elastic (linear elastic for steel and nonlinear elastic for Itamid B-GF35).

2.3.1 FEM Description

The finite element approach used the classical Lagrangian description of the material motion. In this approach, the discretising elements are considered to move with the material. The application of the classical FEM formulation in mechanics results in the following matrix equation[16].

$$[M][\ddot{u}]+[C][\dot{u}]+[K][u]=[F] \tag{3}$$

By taking into account the elastic character of the modelled phenomenon (i.e., small deformations of the material), application of the Lagrangian FEM formulation is reasonable.

The normal contact force between elements of different parts was estimated using a penalty formulation of the contact[17].

$$F_{cont} = 0.1\frac{M_N M_F}{M_N + M_F}\frac{D}{\Delta t^2} \tag{4}$$

For extremely dynamic phenomena (e.g., bullet impact analysis), contact between parts apart the scheme stability criterion is one of main factors determining the time step applied during integration of the equations of motion with an explicit approach. In the case of the slowly changing phenomena under consideration, the main criterion for the time step is the numerical scheme stability condition[17].

$$\Delta t \le CFL\left[\frac{h}{c}\right]_{\min} \tag{5}$$

2.3.2 FEM Basic Numerical Model

The FEM numerical model (Fig. 3) consists of the slide (1), the grip module (2), the barrel (3), the frame (4), the barrel disconnector (5), and the takedown pin (6). The model contains only the parts important for action of the weapon. The grip module was adopted as a small piece that cooperates with the slide as it reaches the rearmost position. The frame was simplified to the runners.

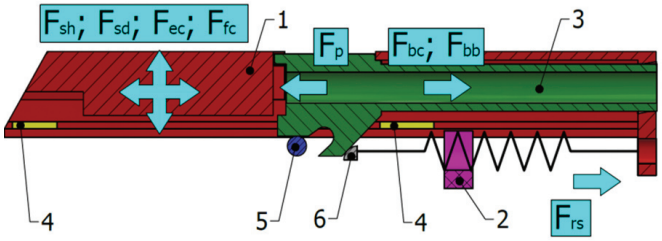

Figure 2. Initial positions of the parts of the FEM base and extended numerical model at time $t = 0$ and the forces acting on the moving elements: 1—slide; 2—grip module; 3—barrel; 4—frame; 5—barrel disconnector; 6—takedown pin.

The system was loaded with the following forces (Fig. 2): F_p, F_{rs}, F_{bc}, and F_{bb}.

The mentioned forces have the same values as in the MBS model, which was described in Section 2.2 and in Badurowicz *et al.*[12]. The recoil spring was treated as a discrete element.

The following initial and boundary conditions were specified:

- Parts of the pistol are stationary at the initial moment $t = 0$
- Material parameters are defined for the parts
- The forces acting on the system are defined
- At the initial moment $t = 0$, the gas pressure starts to increase (which is equivalent to the ignition of propellant); the gas pressure is the input for the system and it forces the motion of parts
- Four stationary parts have fixed support: the grip module (2), the frame (4), the barrel disconnector (5), and the takedown pin (6)
- Five contact pairs are defined: slide (1)—grip module (2), slide (1)—barrel (3), slide (1) —frame (4), barrel (3)—barrel disconnector (5), and barrel (3)—takedown pin (6).

The final considered model was represented by 57,555 nodes and 42,609 hexagonal finite elements. The element characteristic dimensions were between 0.088 and 0.497 mm. When the mesh size was reduced by 50 per cent, the maximum difference of the obtained results was <1 %.

Friction was represented by a Coulomb model described by the following equation[17].

$$\mu = \mu_d + (\mu_s - \mu_d)e^{(-\beta v)} \tag{6}$$

The average time step for the base FEM model was ~35.05 ns, and the total calculation time was 18 hrs, 16 min., and 45 sec. A 4-core/8-thread Intel E5-1620V3 CPU was used for the calculations. The time step safety factor was equal to 0.9.

2.3.3 FEM Extended Numerical Model

The extended numerical model (Fig. 2) consisted of the same six parts as the base model. Its extension consisted in application of additional forces estimated with the MBA approach.

The system was loaded with external forces of the same values as in the base model: F_p, F_{rs}, F_{bc}, and F_{bb}. The following forces were added to the extended model (Fig. 2): F_{sh}, F_{sd}, F_{ec}, and F_{fc}.

The size of the elements in extended model was the same as in the previous approach, and the time step for the extended model was the same as for the base model. The total computation time was 17 hrs, 10 min., and 15 sec. using the same computational resources.

A summary of the main parameters applied during MBA and the FEM is presented in Table 1. The grip module and magazine follower (nonlinear parts) are made of Itamid B-GF35; the other parts are made of steel.

Table 1. Main parameters applied during MBA and FEM simulations

Parameter	MBA value	FEM value
Steel density	7850 kg/m^3	7850 kg/m^3
Steel Young's elastic modulus	—	200 GPa
Brass density	8545 kg/m^3	—
Itamid B-GF35 density	1410 kg/m^3	1410 kg/m^3
Itamid B-GF35 Young's elastic modulus	—	11,500 MPa
Steel–steel static / dynamic friction coefficient	0.15 / 0.08	0.15 / 0.08
Steel–steel β friction coefficient	—	2.749
k_{cont} coefficient	100 N/mm	—
c_{cont} coefficient	10 N s/m	—
e contact coefficient	2.2	—
d contact coefficient	0.01 mm	—
Type of friction coefficient	μ_s	μ_d
Steel–steel	0.15	0.08
Steel–brass	0.11	0.06
Brass–brass	0.10	0.05
Steel–Itamid B-GF35	0.15	0.10
Brass–Itamid B-GF35	0.12	0.08
Type of spring	**Stiffness (N/mm)**	**Preload (N)**
Recoil spring	1.02	23.00
Mainspring	3.70	46.60
Magazine spring	0.35	13.00
Extractor spring	8.83	16.70

3. EXPERIMENTAL TESTS

The laboratory stand used for the experimental tests (Fig. 3) consisted of the investigated pistol and a triangulation displacement sensor (Micro-Epsilon optoNCDT 2300-200, USA) rigidly mounted on the ballistic mount. The plate was screwed to the slide of the weapon to obtain a sufficiently large plane perpendicular to the laser beam, which was necessary for obtaining correct results.

The most important parameters of the triangulation laser displacement sensor are its maximum frequency of 49.14 kHz and its resolution of 3 µm. Experience confirms that such parameters are sufficient for measuring small arms kinematics.

A slide adapted to the mounting of a collimator sight with a cut in its upper part and two threaded holes was used for the tests. Instead of the sight, the plate was mounted with screws. The slide is lighter because of the cut, but, after adding the plate and two screws, its mass is the same as the standard slide mass (i.e., without the cut for a collimator sight).

The tests were conducted using the previously investigated 9×19 mm ammunition with a lead core (Mesko S.A., Poland), and 10 shots were fired. For the series, the average displacement and the average velocity were calculated.

4. RESULTS AND VALIDATION OF THE MBS AND FEM NUMERICAL MODELS

The comparison of the results from the experimental tests and those of numerical investigation using MBS and the FEM are presented by courses of slide displacement versus time (Fig. 4a) and slide velocity versus time (Fig. 4b). Table 2 presents the analysis of the validation of the numerical models.

5. RESULTS OF THE PARAMETRIC NUMERICAL INVESTIGATION

The investigation results for different barrel recoil lengths are shown in Fig. 5 and listed in Table 3. The differences

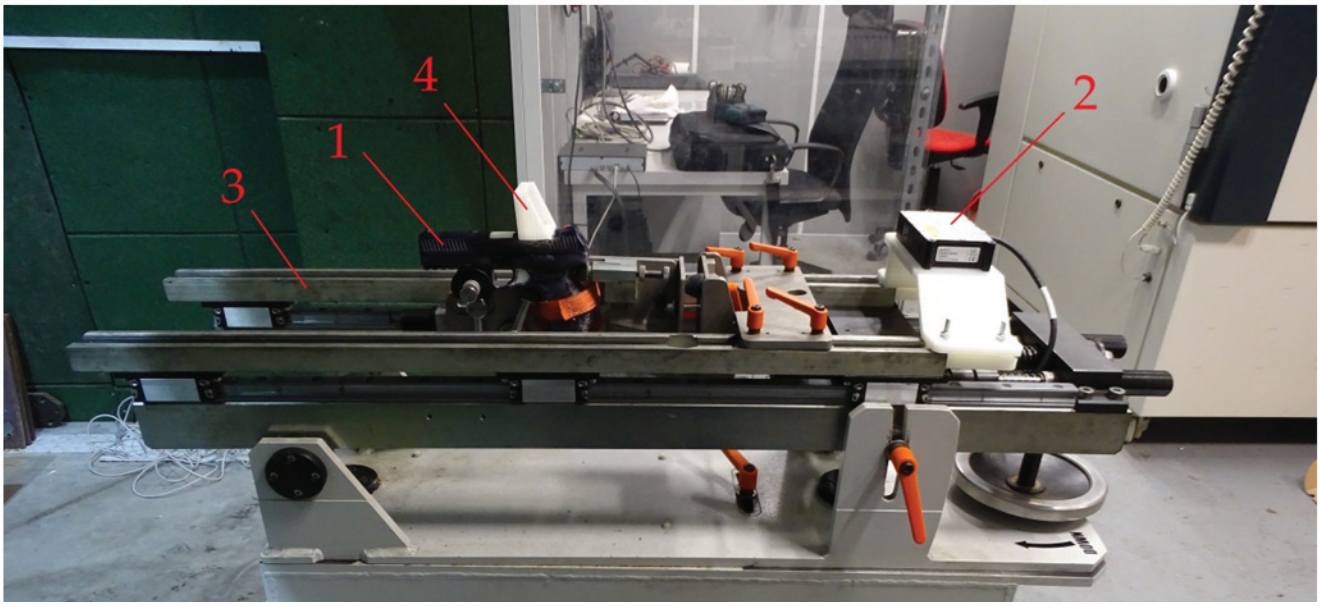

Figure 3. Stand for measuring slide displacement during a shot: 1—weapon; 2—triangulation laser displacement sensor; 3—ballistic mount; 4—plate.

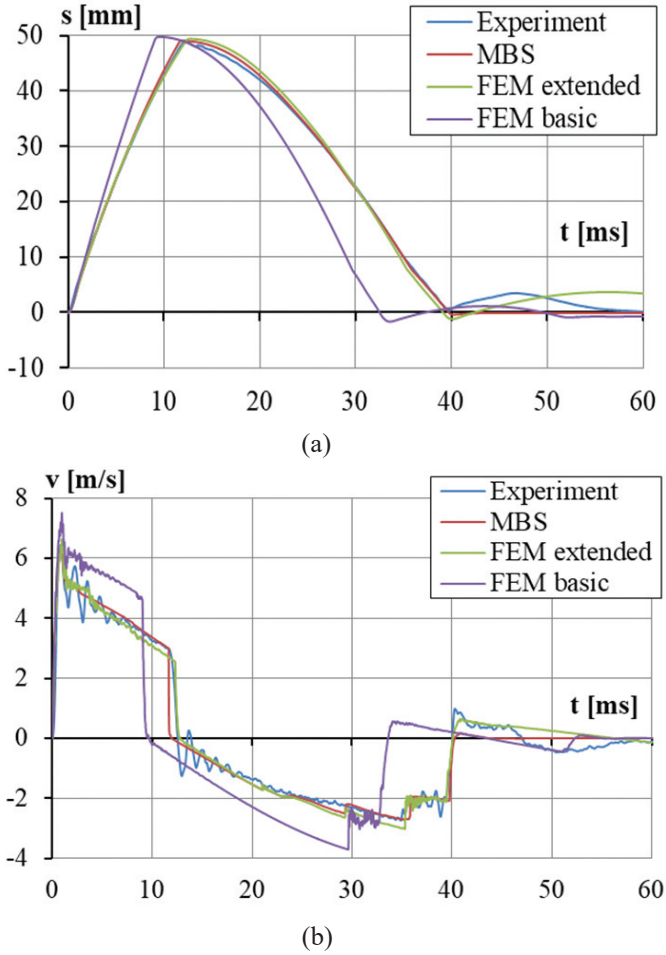

Figure 4. Kinematic characteristics obtained experimentally, using MBS and FEM numerical investigation. (a) Displacement of the slide versus time. (b) Velocity of the slide versus time.

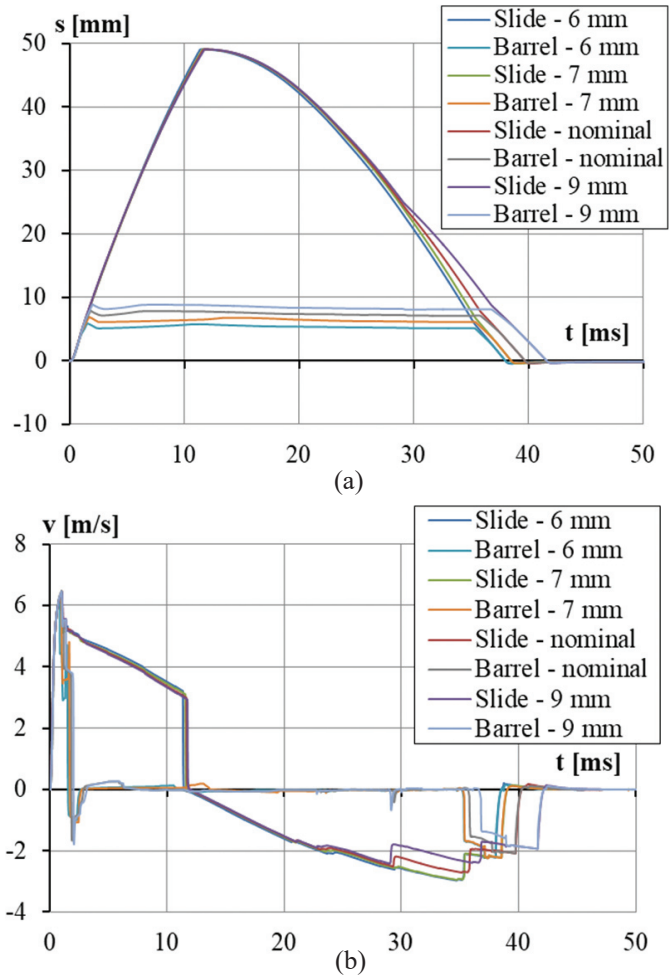

Figure 5. Kinematic characteristics of the slide and barrel for different barrel recoil lengths. (a) Displacement of the slide and barrel versus time. (b) Velocity of the slide and barrel versus time.

Table 2. Analysis of the experimental and numerical results

Type of results	$v_{r\,max}$ **(m/s)**	t_r **(ms)**	v_{sb} **(m/s)**	t_f **(ms)**	$v_{f\,max}$ **(m/s)**
Experiment	6.44	12.57	2.99	2.78	27.43
Standard deviation of experiment	0.19	0.15	0.04	0.10	0.09
Experiment range	0.51	0.43	0.09	0.26	0.24
MBS	6.45	11.90	2.99	2.71	28.40
Difference compared to the experiment	+0.01	−0.67	0.00	−0.07	+0.97
Relative difference	+0.16 %	−5.33 %	0.00 %	−2.52 %	+3.54 %
FEM extended model	6.63	12.74	2.61	3.03	27.32
Difference compared to the experiment	+0.19	+0.17	−0.38	+0.25	−0.11
Relative difference	+2.95 %	+1.35 %	−12.71 %	+8.99 %	−0.40 %
FEM basic model	7.26	10.46	4.13	3.69	24.74
Difference compared to the experiment	+0.82	−2.11	+1.14	+0.91	−2,69
Relative difference	+12.73 %	−16.79 %	+38.13 %	+32.73 %	−9.81 %

: values within the standard deviation of the experiment.
: values within the range of the experiment.
: values not within the range of the experiment (difference between maximum and minimum values) but sufficient for engineering applications, because the range of the gas pressure measurement is 23% (where experimentally obtained gas pressure was used to calculate numerical models).
: values not within the range of the experiment and are of little use for engineering applications.

Table 3. Results of numerical investigation for different barrel recoil displacements

Kinematic characteristics	Barrel recoil displacement			
	6 mm (−2 mm; −25 %)	7 mm (−1 mm; −12.5 %)	Nominal (8 mm)	9 mm (+1 mm; +12.5 %)
$v_{r\max}$ (m/s)	6.28	6.44	6.45	6.45
$\Delta v_{r\max}$ (%)	−2.64	−0.16	0.00	0.00
t_r (ms)	11.5	11.7	11.9	11.9
Δt_r (%)	−3.36	−1.68	0.00	0.00
v_{sb} (m/s)	3.21	3.10	2.99	2.93
Δv_{sb} (%)	+7.36	+3.68	0.00	-2.01
t_f (ms)	2.97	2.95	2.71	2.42
Δt_f (%)	+9.59	+8.86	0.00	−10.70
$v_{f\max}$ (m/s)	27.0	27.3	28.4	30.2
$\Delta v_{f\max}$ (%)	−4.93	−3.87	0.00	+6.34
t_{bo} (ms)	1.27	1.46	1.63	1.82
Δt_{bo} (%)	−22.09	−10.43	0.00	+11.66
t_{ex} (ms)	3.91	4.00	4.02	4.06
Δt_{ex} (%)	−2.74	−0.50	0.00	+1.00
t_{ej} (ms)	2.66	2.17	2.28	2.10
Δt_{ej} (%)	+16.67	−4.82	0.00	−7.89

between the maximum velocity of the slide recoil (v_{rmax}), time of slide recoil (t_r), and velocity of slide impact to the buffer (v_{sb}) are relatively small and they can be ignored in practice. However, the obtained results exhibit greater differences during the slide forward motion (t_f) because of the significant change in resistance during feeding of the next cartridge. This is related to the design of the feeding ramp of the barrel, which was designed for a barrel recoil of 8 mm. It turned out, however, that these resistances are the lowest when the barrel moves 6 mm, which is valuable information for further development work. The decrease in gas pressure to an atmospheric value lasts 1.25 ms[12]. The breech opening time (t_{bo}) is greater than this value, and it is appropriate for each barrel recoil displacement.

6. DISCUSSION

Comparison of the curves obtained by numerical investigation and experimental tests (Fig. 4) reveals qualitative and quantitative similarities. Moreover, the quantitative similarity is shown by the data included in Table 2, demonstrating the efficacy of the applied methods and validity of the stated assumptions. The developed numerical models are extensive and describe the real weapon to an appropriate extent.

Although the basic FEM model does not reflect the real weapon, after importing the forces calculated using MBS, the extended FEM model became highly accurate.

The parametric investigation proved that the barrel recoil displacement could be defined better.

7. CONCLUSIONS

From the above investigations, the following conclusions can be stated:

- The most appropriate (accurate and computationally effective) method of numerical investigation to obtain only the kinematic characteristics of the weapon is MBS, because this method is simpler, faster, and requires fewer computational resources than the FEM.
- The FEM not only allows calculation of kinematic characteristics but also provides stress analysis; however, it requires numerous simplifications to the geometry and limiting the number of weapon parts.
- To obtain more accurate results in FEM simulations, replacing some interactions with force values calculated using MBS is recommended.
- Numerical investigations enable construction of a weapon to be optimised during the design process, reducing the number of models and prototypes and saving both time and money.

REFERENCES

1. Damaziak, K.; Kupidura, P.; Małachowski, J.; Płatek, P.; Woźniak, R. & Zahor, M. Numerical study of modular 5.56 mm standard assault rifle referring to dynamic characteristics. *Def. Sci. J.*, 2015, **65**(6), 431-437. doi: 10.14429/dsj.65.8259
2. Fikus, B. & Trębiński, R. Numerical simulation of submachine gun operation cycle. *In* Proceedings of International Scientific Conference 'Defense Technologies' DefTech, Faculty of Artillery, Air Defense and Communication and Information Systems, 2020.
3. Fikus, B.; Płatek, P.; Surma, Z. & Trębiński, R. Preliminary numerical and experimental investigations of 9 mm pistol bullet and barrel interaction. *In* Conference: 31st

International Symposium on ballistics, 2019.
doi: 10.12783/ballistics2019/33068
4. Szmit, Ł.; Leciejewski, Z.; Kijewski, J. Preliminary theoretical and experimental studies at the recoil and weapon's jump of the automatic firearms. *University Review*, 2013, **7**(4), 38-46.
5. Goździk, D.; Kijewski, J.; Kupidura, P. & Szmit, Ł. Influence of muzzle device on the jump of some rifles of msbs-5.56 modular small arms system and the accuracy of shot pattern. *Issues Armament Technol.*, 2019, **150**(2), 45-57.
doi: 10.5604/01.3001.0013.5896
6. Szmit, Ł. & Woźniak, R. Specificity of design and action of the weapon's jump and recoil laboratory test stand. *Problems of Mechatronics*, 2012, **3**(3), 29-39.
7. Ni, J.; Wang X. & Xu, Ch. Virtual test technology study of automatic weapon. *World J. Modell. Simul.*, 2011, **7**(2), 155-160.
8. Rodriguez, C. Mechanical system simulation of the XM307 advanced crew served weapon. *In* National Defence Industrial Association Joint Services Small Arms Systems Annual Symposium, 2007.
9. Benelli Armi S.p.A. Developing new customizable armament. MSC.Software Case Study, 2012.
10. Ozmen, D.; Kurt, M.; Ekici, B. & Kaynak, Y. Static, dynamic and fatigue analysis of a semi-automatic gun locking block. *Engineering Failure Analysis*, 2006, **16**, 2235-2244.
doi:10.1016/j.engfailanal.2009.03.014
11. Hopkins, D.A. Modeling gun dynamics with three dimensional beam elements. *In* Sixth U.S. Army Symposium on gun dynamics volume I of II, 1990.
12. Badurowicz, P.; Fikus, B.; Kupidura, P. & Stępniak, W. Development of the preliminary numerical model of the short recoil operated weapon using the multibody systems. *Problems of Mechatronics*, 2021, **12**(1), 27-40.
doi: 10.5604/01.3001.0014.7849
13. Frączek, J. & Wojtyra, M. Kinematics of multibody systems. Computational methods (in Polish). Scientific and Technical Publishers, 2008.
14. South, J.; Yiournas, A.; Wagner, J.; Brown, J. & Kaste, R. A study of the engraving of the M855 5.56-mm Projectile. army research laboratory, 2009, Report - ARL-TR-4743.
15. Kowalczyk, A.; Stępniak, W. & Kaczmarski, S. Experimental and analytical method of determining the resistance of a bullet engraving into a barrel. *Issues Armament Technol.*, 2000, **29**(75), 73-87.
16. Rakowski, G. & Kacprzyk, Z. Finite element method in structural mechanics (in Polish). Publishing House of the Warsaw University of Technology, 2005.
17. Ansys help. https://www.ansyshelp.ansys.com/ (Accessed on 28 December 2020).

CONTRIBUTORS

Mr Przemysław Badurowicz, MSc, is a Scientific Assistant at the Ballistic Department of the Military Institute of Armament Technology in Zielonka, Poland. He graduated from the Military University of Technology in Warsaw, Poland. His area of research is firearms.
Contribution to the current study: Conceptualisation, methodology, software, validation, formal analysis, investigation, resources; data curation, writing - original draft preparation, visualisation.

Dr Przemysław Kupidura, PhD, D.Sc. (Eng.), is a Deputy Dean of the Faculty of Mechatronics, Armament and Aerospace of the Military University of Technology in Warsaw. His area of research is firearms.
Contribution to the current study: Conceptualisation, methodology, formal analysis, writing - review and editing, supervision, project administration.

Dr Bartosz Fikus obtained his PhD at the Faculty of Mechatronics, Armament and Aerospace of the Military University of Technology in Warsaw, where he currently works as an Assistant Professor. His areas of research include: Firearms and numerical and experimental investigations of internal and terminal ballistics problems.
Contribution to the current study: Conceptualisation, methodology, validation, formal analysis, writing - original draft preparation, review and editing, supervision, and project administration.